

Unbalanced Incomplete Multi-view Clustering via the Scheme of View Evolution: Weak Views are Meat; Strong Views do Eat

Xiang Fang, Yuchong Hu, *Member, IEEE*, Pan Zhou, *Member, IEEE*, Xiao-Yang Liu, *Graduate Student Member, IEEE*, and Dapeng Oliver Wu, *Fellow, IEEE*

Abstract—Incomplete multi-view clustering is an important technique to deal with real-world incomplete multi-view data. Previous works assume that all views have the same incompleteness, i.e., balanced incompleteness. However, different views often have distinct incompleteness, i.e., unbalanced incompleteness, which results in *strong views* (low-incompleteness views) and *weak views* (high-incompleteness views). The unbalanced incompleteness prevents us from directly using the previous methods for clustering. In this paper, inspired by the effective biological evolution theory, we design the novel scheme of *view evolution* to cluster strong and weak views. Moreover, we propose an Unbalanced Incomplete Multi-view Clustering method (UIMC), which is the *first* effective method based on view evolution for unbalanced incomplete multi-view clustering. Compared with previous methods, UIMC has two unique advantages: 1) it proposes weighted multi-view subspace clustering to integrate these unbalanced incomplete views, which effectively solves the unbalanced incomplete multi-view problem; 2) it designs the low-rank and robust representation to recover the data, which diminishes the impact of the incompleteness and noises. Extensive experimental results demonstrate that UIMC improves the clustering performance by up to 40% on three evaluation metrics over other state-of-the-art methods.

Index Terms—Unbalanced incomplete multi-view clustering, weak view, strong view, view evolution.

I. INTRODUCTION

Real data are often with multiple modalities [1]–[5] or collected from different sources [6]–[14], which are called multi-view data [15]–[20]. In many real-world datasets, some views often lose some instances, which results in incomplete views [4]. As an illustration, for a multilingual document clustering task, different languages of a document represent distinct views, but we may not translate each document into all languages [21]–[23]. The incompleteness will reduce the information available for clustering, which hurts clustering performance. Due to the ability to integrate these incomplete

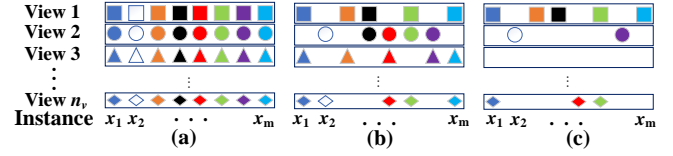


Fig. 1: Different types of multi-view data, where (a) is complete multi-view data (all views have no missing instances), (b) is balanced incomplete multi-view data (different views have the same number of missing instances), and (c) is unbalanced incomplete multi-view data (different views have the distinct number of missing instances).

views, incomplete multi-view clustering has attracted more and more attention [24], [25].

Recently, some incomplete multi-view clustering methods have been proposed. [26] proposes PVC to learn a common latent subspace for all incomplete views. To couple the incomplete multi-view instances, [27] proposes IMG by integrating the latent subspace generation and the compact global structure into a unified framework. To handle the situation of multiple incomplete views, [28] proposes MIC by integrating the joint weighted nonnegative matrix factorization [29] and $L_{2,1}$ regularization. To reduce the deviation when the missing rate is large, [21] proposes DAIMC by considering the instance alignment information and aligning different basis matrices simultaneously. To learn the common representation for incomplete multi-view clustering, [30] proposes IMSC_AGL by exploiting the graph learning [31]–[33] and spectral clustering techniques. To obtain the robust clustering results, UEAF [34] performs the unified common embedding aligned with incomplete views inferring framework.

However, almost all incomplete multi-view clustering methods use the view alignment technology for clustering. When using the technology, they always assume that each view has the same incompleteness (called *balanced* incompleteness in Fig. 1(b)) and ignore that different views often have distinct incompleteness (called *unbalanced* incompleteness in Fig. 1(c)). For convenience, we name the view with low incompleteness as *strong view* and the view with high incompleteness as *weak view*. But real-world incomplete multi-view data are often unbalanced incomplete, rather than balanced incomplete. For example, in web page clustering, different types of data, such as hyper-links, texts, images, and videos, can be regarded as different views, and most web pages (e.g., Google Scholar and arXiv) only have hyper-links and

X. Fang is with the School of Computer Science and Technology, Huazhong University of Science and Technology, Wuhan 430074, China (e-mail: xfang9508@gmail.com).

Y. Hu is with the School of Computer Science and Technology, Huazhong University of Science and Technology, Wuhan 430074, China (e-mail: yuchonghu@hust.edu.cn).

P. Zhou is with the Hubei Engineering Research Center on Big Data Security, School of Cyber Science and Engineering, Huazhong University of Science and Technology, Wuhan 430074, China (e-mail: panzhou@hust.edu.cn).

X. Y. Liu is with the Department of Electrical Engineering, Columbia University, New York, NY 10027 USA (e-mail: xl2427@columbia.edu).

D. O. Wu is with the Department of Electrical and Computer Engineering, University of Florida, Gainesville, FL 32611 USA (e-mail: dpwu@ieee.org).

texts (which are strong views) but not images and videos (which are weak views). Thus, real-world incomplete multi-view data are often unbalanced incomplete, rather than balanced incomplete. Unfortunately, previous incomplete multi-view clustering methods cannot directly integrate unbalanced incomplete views. It is because these views have different numbers of presented instances, even some views have no instance (e.g., View 3 in Fig. 1(c)). The unbalanced incompleteness makes these methods unable to align different views for clustering. Therefore, unbalanced incomplete multi-view clustering remains unexplored.

In this paper, we propose an Unbalanced incomplete Multi-view Clustering method (UIMC) to explore the problem. By integrating weighted multi-view subspace clustering (weighted MVSC) and the low-rank and robust representation, UIMC minimizes the disagreement between each cluster indicator matrix and the consensus, and adaptively learns the proper weights for strong and weak views. The contributions of UIMC mainly include:

- As far as we know, UIMC is a *pioneering* work by introducing the biological evolution theory into clustering algorithms, which has the potential to stimulate new biological ideas and findings in machine learning tracks. Moreover, inspired by biological evolution, UIMC might be the *first* effective method by proposing the scheme of view evolution for unbalanced incomplete multi-view clustering.
- By designing weighted MVSC, UIMC directly integrates unbalanced incomplete views by structuring their Laplacian graphs and weighting these views, which decreases the impact of unbalanced incompleteness. Also, UIMC minimizes the disagreement between each cluster indicator matrix and the consensus cluster indicator matrix, which aligns the same instances in different views. Besides, UIMC quantifies the contributions of strong and weak views by weighting each view properly based on its incompleteness, which makes full use of these presented instances for clustering.
- With the help of the low-rank and robust representation, UIMC recovers the data structure for clustering by Γ -norm and $L_{2,1}$ -norm, which further reduces the influence of incompleteness and noises.
- Experimental results on four real-world datasets demonstrate its superiority over state-of-the-arts. Impressively, based on three evaluation metrics, it raises the clustering performance by more than 40% in representative cases.

The rest of the paper is organized as follows. Section II describes the notations and the related works. Section III first motivates UIMC's main idea, then proposes UIMC, and finally solves it efficiently. Section IV evaluates UIMC's performance. Section V concludes the paper.

II. NOTATIONS AND RELATED WORKS

We first define the notations used throughout the paper and then describe three relevant works.

Notation: Given an original dataset $\{\bar{\mathbf{X}}^{(v)} \in \mathbb{R}^{d_v \times m}, v = 1, \dots, n_v\}$ with n_v views, m instances, and $\bar{\mathbf{X}}^{(v)}$ is the v -th

view matrix and d_v is the feature dimension of $\bar{\mathbf{X}}^{(v)}$. We can extract these presented instances from the original view matrix $\bar{\mathbf{X}}^{(v)}$ and update it to a new view matrix $\mathbf{X}^{(v)} \in \mathbb{R}^{d_v \times k_v}$, which has k_v instances. $\mathbf{M}^{(v)} \in \mathbb{R}^{m \times k_v}$ is an indicator matrix to represent the update. $\mathbf{1}$ is a column vector with all the elements as one; $\mathbf{0}$ is a zero matrix; \mathbf{I} is the identity matrix. For the view matrix $\mathbf{X}^{(v)}$, w_v is its weight, $\mathbf{E}^{(v)} \in \mathbb{R}^{d_v \times k_v}$ is its error matrix, $\mathbf{A}^{(v)} \in \mathbb{R}^{k_v \times k_v}$ is its subspace matrix, $\mathbf{F}^{(v)} \in \mathbb{R}^{m \times c}$ is its cluster indicator matrix (where c is the cluster number), $\mathbf{F}^* \in \mathbb{R}^{m \times c}$ is its consensus cluster indicator matrix. $\|\cdot\|_\Gamma$ is the Γ -norm; $\|\cdot\|_1$ is the L_1 -norm; $\|\cdot\|_F$ is the Frobenius norm; $\|\cdot\|_{2,1}$ is the $L_{2,1}$ -norm. θ is a penalty parameter and we set $\theta=0.01$ in this paper. α, β and η are nonnegative hyper-parameters, each of which is a trade-off between two specific objectives.

Unbalanced incomplete multi-view clustering is a problem of clustering incomplete multi-view data, where at least two views have different missing rates.

Definition 1. (Strong view, weak view and dying view). For the $\{v\}_{v=1}^{n_v}$ -th view matrix $\bar{\mathbf{X}}^{(v)}$, r_v denotes the missing rate. $\bar{\mathbf{X}}^{(v)}$ is the strong view if its missing rate is less than the average ($r_v < (r_1 + r_2 + \dots + r_{n_v})/n_v$). $\bar{\mathbf{X}}^{(v)}$ is the weak view if its missing rate is greater than the average ($r_v > (r_1 + r_2 + \dots + r_{n_v})/n_v$). $\bar{\mathbf{X}}^{(v)}$ is the dying view if the number of presented instances is fewer than the number of clusters ($m \times (1 - r_v) < c$).

A. Unbalanced Incomplete Multi-view Data

For an incomplete multi-view dataset, the v -th original view matrix (including missing and presented instances) is represented as $\bar{\mathbf{X}}^{(v)} \in \mathbb{R}^{d_v \times m}$, where d_v is the feature dimension and m is the instance number. By removing the columns with missing instances from the view matrix (i.e., preserving these presented instances), we can update the v -th original view matrix to a new view matrix $\mathbf{X}^{(v)} \in \mathbb{R}^{d_v \times m_v}$, where m_v is the number of presented instances ($m_v < m$). To represent the update, we leverage an indicator matrix $\mathbf{M}^{(v)} \in \mathbb{R}^{m_v \times m}$ defined as:

$$\mathbf{M}_{i,j}^{(v)} = \begin{cases} 1, & \text{if the } \mathbf{X}_i^{(v)} \text{ is in } \bar{\mathbf{X}}_j^{(v)}; \\ 0, & \text{otherwise,} \end{cases} \quad (1)$$

where $\bar{\mathbf{X}}_j^{(v)}$ is the j -th column of $\bar{\mathbf{X}}^{(v)}$, and $\mathbf{X}_i^{(v)}$ is the i -th column of $\mathbf{X}^{(v)}$, which is the v -th updated view matrix.

B. Multi-view Subspace Clustering

As a classic complete multi-view clustering method, multi-view subspace clustering (MVSC) tries to obtaining a cluster indicator matrix for clustering [35]. For a complete multi-view dataset $\{\bar{\mathbf{X}}\}_{v=1}^{n_v}$, MVSC is formulated as:

$$\begin{aligned} J = & \min_{\mathbf{A}^{(v)}, \mathbf{E}^{(v)}, \mathbf{F}} \sum_v (\|\bar{\mathbf{X}}^{(v)} - \bar{\mathbf{X}}^{(v)} \mathbf{A}^{(v)} - \mathbf{E}^{(v)}\|_F^2 \\ & + \beta \|\mathbf{E}^{(v)}\|_1 + \eta \text{Tr}(\mathbf{F}^T \mathbf{L}_A^{(v)} \mathbf{F})) \\ \text{s.t. } & \mathbf{F} \mathbf{F}^T = \mathbf{I}, \mathbf{A}^{(v)T} \mathbf{1} = \mathbf{1}, \mathbf{A}_{i,i}^{(v)} = 0, \end{aligned} \quad (2)$$

where for view v , $\mathbf{L}_A^{(v)}$ is its Laplacian graph, $\mathbf{E}^{(v)}$ is its error matrix, and $\mathbf{L}_A^{(v)}$ is its Laplacian graph, $\mathbf{A}^{(v)}$ is its subspace matrix, $\mathbf{A}_{i,i}^{(v)} = 0$ means that each diagonal elements of \mathbf{A} is 0; \mathbf{F} is the cluster indicator matrix. However, MVSC can only cluster complete multi-view data. When dealing with incomplete multi-view data, MVSC will fail due to the inability to learn the cluster indicator matrix from incomplete view matrix.

C. Biological Evolution Theory

Biological evolution theory is an effective method to analyze the impact of different biological traits on biological population development. “Survival of the fittest” [36] is a milestone work of the biological evolution theory. As a milestone work of the biological evolution theory, “Survival of the fittest” is proposed by Herbert Spencer [36]. Based on this work, Darwin proposed Darwin’s theory of evolution [37], whose key idea is the natural selection. For a biological population, the natural selection function (J_g) is formulated as

$$J_g = \sum_{v=1}^{n_t} a_v \mathbf{T}^{(v)}, \quad (3)$$

where n_t is the number of biological traits; $\mathbf{T}^{(v)}$ is the v -th trait matrix; a_v is the weight of $\mathbf{T}^{(v)}$ and a_v quantifies the influence of $\mathbf{T}^{(v)}$ on biological population development.

The directional selection differential is

$$\Delta^t a_v = a_v^t - a_v^{t-1}, \quad (4)$$

where a_v^t is the weight of $\mathbf{T}^{(v)}$ after the t -th selection; a_v^{t-1} is the weight of $\mathbf{T}^{(v)}$ before the t -th selection. If $\Delta^t a_v > 0$, $\mathbf{T}^{(v)}$ is the strong trait; if $\Delta^t a_v < 0$, $\mathbf{T}^{(v)}$ is the weak trait. When the proportion of a trait is much smaller than the average $1/n_t$, the trait (we call it *dying trait*) often disappears. Therefore, we can visually describe the selection as: “The weak are meat, and the strong do eat!” [38].

III. SCHEME OF VIEW EVOLUTION

We first present the motivation for proposing the scheme of view evolution, then explain the challenges encountered, and finally meet the challenge.

A. Motivation

By learning a consensus matrix shared by all views (denoted by \mathbf{C}), previous incomplete multi-view clustering methods can align balanced incomplete views for clustering. But many real-world datasets often contain unbalanced incomplete views as shown in Fig. 1(c) where view 1, 2 and 3 have three, six and eight missing instances, respectively. Thus, these unbalanced incomplete view matrices $\{\mathbf{X}^{(v)}\}_{v=1}^{n_v} \in \mathbb{R}^{d_v \times k_v}$ have distinct numbers of columns and rows, which make it difficult for previous methods to obtain the consensus matrix (i.e., \mathbf{C}) shared by all views for view alignment. Thus, different view

matrices lose distinct numbers of rows or columns and the unbalanced incompleteness will make it difficult for these methods to obtain available \mathbf{C} . What is worse, when a view has no instances (i.e., View 3 in Fig. 1(c)), these methods will fail during matrix calculation because no instance on the view can be used for calculation. Also, these methods assume that different views have the same contribution to clustering. But different views will have unbalanced contributions for clustering because they have different numbers of presented instances. The unbalanced contributions will make these methods unable to make full use of the presented instance information, which makes these methods difficult to obtain satisfactory clustering performance.

In Eq. (3), the biological evolution theory integrates strong and weak traits by assigning a weight to each trait. Inspired by the theory, to integrate strong and weak views, we propose the scheme of view evolution “weak views are meat; strong views do eat”. An intuitive idea on the scheme is to directly assign a proper weight to each view (similar to Eq. (3)), and then linearly superimpose the objective function of each view. However, when implementing this idea, we have the following challenges: 1) how to bridge unbalanced incomplete views (i.e., construct view representations with the same matrix size for different views); 2) how to group similar instances on each view; 3) how to quantify the contribution of each view; 4) how to update the contribution. In the next section, we will meet these challenges.

B. Weighted MVSC

1) Bridging unbalanced incomplete views by constructing Laplacian graphs: When directly using MVSC to process an unbalanced dataset $\{\mathbf{X}^{(v)}\}_{v=1}^{n_v} \in \mathbb{R}^{d_v \times k_v}$, we will obtain these subspace matrices $\{\mathbf{Z}^{(v)}\}_{v=1}^{n_v} \in \mathbb{R}^{k_v \times k_v}$ with different matrix sizes. Since k_v is different for these views, it is difficult to directly deal with these subspaces for view bridge. To facilitate view bridge, we construct the following Laplacian graph as the view representation

$$\mathbf{M}^{(v)T} \mathbf{L}_A^{(v)} \mathbf{M}^{(v)} = \mathbf{D}_A^{(v)} - \mathbf{W}_A^{(v)}, \quad (5)$$

where $\mathbf{D}_{A,i,i}^{(v)} = \sum_j \mathbf{W}_{A,i,j}^{(v)}$ and $\mathbf{W}_A^{(v)} = (|\mathbf{M}^{(v)T} \mathbf{A}^{(v)} \mathbf{M}^{(v)}| + |\mathbf{M}^{(v)T} \mathbf{A}^{(v)T} \mathbf{M}^{(v)}|)/2$. Note that the Laplacian graph $\mathbf{M}^{(v)T} \mathbf{L}_A^{(v)} \mathbf{M}^{(v)} \in \mathbb{R}^{m \times m}$. Since m is constant, the Laplacian graphs of different views have same matrix size, which can be used to bridge unbalanced incomplete views.

2) Aligning views by introducing the disagreement function: Aligning the same instances in different views is the goal of bridging unbalanced incomplete views. We align different views based on the cluster indicator matrix, which represents the relationship between instances and clusters. Based on the relationship, we can group similar instances into one cluster. We assume that the v -th cluster indicator matrix $\mathbf{F}^{(v)}$ is a perturbation of the consensus cluster indicator matrix \mathbf{F}^* . To reduce further the negative influence of the perturbation, we align the same instances in different views by minimizing the

¹“Meat” and “eating” do not mean a predator relationship, but a competitive relationship (or strong biological traits eat the weights of the weak biological traits).

disagreement between $\mathbf{F}^{(v)}$ and \mathbf{F}^* . We leverage the following disagreement function: $d(\mathbf{F}^*, \mathbf{F}^{(v)})$

$$d(\mathbf{F}^*, \mathbf{F}^{(v)}) = \left\| \frac{\mathbf{F}^{(v)} \mathbf{F}^{(v)T}}{\|\mathbf{F}^{(v)} \mathbf{F}^{(v)T}\|_F^k} - \frac{\mathbf{F}^* \mathbf{F}^{*T}}{\|\mathbf{F}^* \mathbf{F}^{*T}\|_F^k} \right\|_F^2, \quad (6)$$

where k is an any positive integer, $\mathbf{F}^{(v)} \mathbf{F}^{(v)T}$ is the similarity matrix of $\mathbf{F}^{(v)}$, and $\mathbf{F}^* \mathbf{F}^{*T}$ is the similarity matrix of \mathbf{F}^* . Since $\|\mathbf{F}^{(v)} \mathbf{F}^{(v)T}\|_F^2 = \|\mathbf{F}^* \mathbf{F}^{*T}\|_F^2 = c$, we rewrite Eq. (6) as:

$$d(\mathbf{F}^*, \mathbf{F}^{(v)}) = \frac{2c - 2\text{Tr}(\mathbf{F}^* \mathbf{F}^{*T} \mathbf{F}^{(v)} \mathbf{F}^{(v)T})}{c^k}. \quad (7)$$

3) Integrating views by weighting them: The alignment in Eq. (7) cannot quantify the contribution of each view to clustering. Since strong views have more presented instances and lower incompleteness than weak views, strong views often contain more available data information and have greater contributions. To make full use of the information for clustering, we give strong views larger weights than weak views (larger weight means greater contribution). To judge the contribution of the v view, we design the following weight w_v based on the incompleteness

$$w_v = \begin{cases} 0, & \text{if } k_v < c; \\ \frac{\sum_i \sum_j \mathbf{M}_{i,j}^{(v)}}{\sum_v \sum_i \sum_j \mathbf{M}_{i,j}^{(v)}} \times n_v, & \text{otherwise,} \end{cases} \quad (8)$$

where $\sum_i \sum_j \mathbf{M}_{i,j}^{(v)}$ denotes the number of presented instances in the v -th view, $\sum_v \sum_i \sum_j \mathbf{M}_{i,j}^{(v)}$ denotes the total number of present instances in all views. For the case $k_v < c$ (i.e., view v is a dying view) in Eq. (8), it is incapable to divide k_v instances into c clusters. To learn available weights for unbalanced incomplete views, we remove dying views by assigning them zero weights. When we perform clustering, these views with $w_v=0$ will be removed. If the number of removed views is t_v , we will update n_v to $n_v - t_v$. Since strong views have more presented instances than weak views, strong views often contain more data information. To make full use of the presented data information for clustering, we give strong views larger weights than weak views in Eq. (8).

4) Updating weights: To update each weight adaptively, we leverage an iterative optimization procedure (see Section III-E in more detail). After each iteration, we can update the weight w_v as follows:

$$w_v = \min(\mu w_v, w_{max}), \quad (9)$$

where w_{max} is the upper bound of w_v ($w_{max} < n_v$) and μ is a nonnegative coefficient of updating w_v . Based on the effect of μ on the weight, we divide the update into two types:

$$\text{The update is } \begin{cases} \text{favorable,} & \text{if } \mu > 1; \\ \text{harmful,} & \text{if } 0 < \mu < 1. \end{cases} \quad (10)$$

Combining Eq. (9) and Eq. (10), we can notice that the favorable update will increase the weight and the harmful update will decrease the weight. To improve the clustering results, we give strong views larger μ than the weak views at each iteration (In our experiment, we set $\mu=1.1$ for strong views and $\mu=0.9$ for weak views, and our experiment results show the effectiveness of this setting). Therefore, *after each*

iteration, the weights of strong views will increase, while the weights of weak views will decrease. We call this phenomenon “strong views eat the weights of weak views”.

5) Relation to biological evolution : For simplicity, we introduce Lemma 1.

Lemma 1. *For any two positive numbers a and b , $a - b > 0$ is equivalent to $a/b > 1$.*

If we correspond each view to a trait in Eq. (3), we can find the following interesting phenomenon based on Eq. (4): the weights of strong traits will increase after one selection, while the weights of strong views will also increase after one iteration. The dying traits will disappear due to the natural selection, while the dying views will be removed via Eq. (8). Therefore, the scheme of view evolution can be viewed as an extension from the biological evolution to clustering.

Combining Eq. (2), Eq. (8) and Eq. (7), the final model of our weighted MVSC is as follows:

$$\begin{aligned} \min_{\mathbf{A}^{(v)}, \mathbf{E}^{(v)}, \mathbf{F}^{(v)}, \mathbf{F}^*} \quad & \sum_v (w_v \|\mathbf{X}^{(v)} - \mathbf{X}^{(v)} \mathbf{A}^{(v)} - \mathbf{E}^{(v)}\|_F^2 \\ & + \beta \|\mathbf{E}^{(v)}\|_1 + \eta \text{Tr}(\mathbf{F}^{(v)T} \mathbf{M}^{(v)T} \mathbf{L}_A^{(v)} \mathbf{M}^{(v)} \mathbf{F}^{(v)}) \\ & - \alpha \text{Tr}(\mathbf{F}^* \mathbf{F}^{*T} \mathbf{F}^{(v)} \mathbf{F}^{(v)T})) \\ \text{s.t. } \quad & \mathbf{F}^{(v)T} \mathbf{F}^{(v)} = \mathbf{I}, \mathbf{F}^{*T} \mathbf{F}^* = \mathbf{I}, \mathbf{A}^{(v)} \mathbf{1} = 1, \mathbf{A}_{i,i}^{(v)} = 0, \end{aligned} \quad (11)$$

where c and k are constants, and we ignore them in Eq. (11). Note that Eq. (11) only integrates different views structurally, and it is difficult to recover and denoise the incomplete data because no related technology is used. When a dataset has high incompleteness and several noises, Eq. (11) may obtain unsatisfactory clustering performance. In the next section, we will design the low-rank and robust representation model to recover and denoise the incomplete data.

C. Low-rank and Robust Representation

1) Low-rank representation via Γ -norm: For a real-world incomplete data, the low-rank representation is an effective method to recover the underlying true low-rank data matrix. The low-rank representation of the subspace is widely used in many subspace-based clustering approaches to improve the clustering performance [39]–[42]. Most of these approaches assume that the nuclear norm of coefficient matrix ($\|\cdot\|_*$) is balanced to the rank of the coefficient matrix ($\text{rank}(\cdot)$). However, the results obtained with this assumption may deviate significantly from the truth [43]. Therefore, a reasonable low-rank representation of subspace can improve the clustering performance. γ -norm [43] is a state-of-the-art nonconvex low-rank representation method, which can get more accurate results than the nuclear norm used by most clustering methods. However, γ -norm can only handle single view data. To obtain a satisfactory low-rank representation, we design the Γ -norm $\|\mathbf{A}^{(v)}\|_\Gamma$ of $\mathbf{A}^{(v)}$ as follows:

$$\|\mathbf{A}^{(v)}\|_\Gamma = \sum_{i=1}^{k_v} \frac{\epsilon_i^{(v)}}{\epsilon_i^{(v)} + \gamma}, \quad (12)$$

where $\mathbf{A}^{(v)} \in \mathbb{R}^{k_v \times k_v}$, γ is a penalty parameter and $\epsilon_i^{(v)}$ is the i -th singular value of $\mathbf{Z}^{(v)}$. Note that if $\gamma \rightarrow 0$,

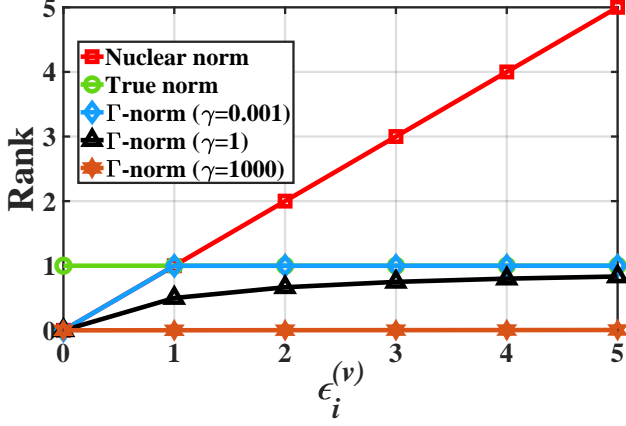


Fig. 2: The performance of different functions to the rank w.r.t. a varying positive singular value $\epsilon_i^{(v)}$ (True rank is 1).

$\|A^{(v)}\|_G \rightarrow \text{rank}(A^{(v)})$, and we choose a small γ (e.g., $\gamma = 0.001$). Fig. 2 compares the rank approximation performance of the nuclear norm and our designed Γ -norm with different γ . Obviously, Γ -norm with $\gamma = 0.001$ is closer to the true rank than the nuclear norm.

2) Robustness based on $L_{2,1}$ -norm: To reduce the influence of noises, we replace L_1 -norm in Eq. (11) with a relaxed regularization $L_{2,1}$ -norm that is robust to noises. $L_{2,1}$ -norm of $E^{(v)}$ is defined as:

$$\|E^{(v)}\|_{2,1} = \sum_{i=1}^{d_v} \sqrt{\sum_{j=1}^{k_v} |E_{ij}^{(v)}|^2}. \quad (13)$$

Combining Eq. (12) and Eq. (13), the low-rank and robust representation model is as follows:

$$\min_{A^{(v)}, E^{(v)}} \|A^{(v)}\|_G + \beta \|E^{(v)}\|_{2,1}. \quad (14)$$

D. Objective Function

Integrating weighted MVSC (i.e., Eq. (11)) and low-rank and robust representation (i.e., Eq. (14)), we can obtain final objective function:

$$\begin{aligned} L = & \min_{A^{(v)}, E^{(v)}, F^{(v)}, F^*} \sum_v (\|A^{(v)}\|_G + w_v \theta \|X^{(v)} - X^{(v)} A^{(v)} \\ & - E^{(v)}\|_F^2 + \eta \text{Tr}(F^{(v)T} M^{(v)T} L_A^{(v)} M^{(v)} F^{(v)}) \\ & - \alpha \text{Tr}(F^* F^{*T} F^{(v)} F^{(v)T}) + \beta \|E^{(v)}\|_{2,1}) \\ \text{s.t. } & F^{(v)T} F^{(v)} = I, F^{*T} F^* = I, A^{(v)} \mathbf{1} = 1, A_{i,i}^{(v)} = 0, \end{aligned} \quad (15)$$

where α, β and η are nonnegative hyper-parameters, which are used to control the trade-off between two objectives. θ is a penalty parameter. Note that Eq. (15) is a nonconvex function, which is often difficult to optimize. In the next section, we will design an iteration procedure to optimize it.

E. Optimization of Evolution

To simplify the optimization of Eq. (15), we design the following augmented Lagrangian function

$$\begin{aligned} J = & \sum_v (\|Q_1^{(v)}\|_G - \alpha \text{Tr}(F^* F^{*T} F^{(v)} F^{(v)T}) + \beta \|E^{(v)}\|_{2,1} \\ & + \vartheta^{(v)T} (1 - Q_2^{(v)} \mathbf{1}) + \frac{w_v \theta}{2} (\|X^{(v)} - X^{(v)} A^{(v)} - E^{(v)} \\ & + \frac{H_0^{(v)}}{w_v \theta} \|F\|_F^2 + \|A^{(v)} - Q_1^{(v)} + \frac{H_1^{(v)}}{w_v \theta} \|F\|_F^2 + \|A^{(v)} - Q_2^{(v)} \\ & + \frac{H_2^{(v)}}{w_v \theta} \|F\|_F^2) + \eta \text{Tr}(F^{(v)T} M^{(v)T} L_{Q_2}^{(v)} M^{(v)} F^{(v)})), \end{aligned} \quad (16)$$

where $H_0^{(v)}, H_1^{(v)}, H_2^{(v)}$ and $\vartheta^{(v)}$ are Lagrange multipliers. Note that Eq. (16) is not convex for all variables simultaneously (it is actually non-convex), and it is difficult to solve Eq. (16) in one step. Thus, we design the following nine-step procedure to update each variable iteratively [43].

Step 1. Updating $F^{(v)}$. Fixing the other variables, for the update of $F^{(v)}$, we need to minimize:

$$\begin{aligned} J(F^{(v)}) = & \eta \text{Tr}(F^{(v)T} Y^{(v)} F^{(v)}) - \alpha \text{Tr}(Z F^{(v)} F^{(v)T}) \\ \Rightarrow J(F^{(v)}) = & \text{Tr}(F^{(v)T} (\eta Y^{(v)} - \alpha Z) F^{(v)}), \end{aligned} \quad (17)$$

where $Y^{(v)} = M^{(v)T} L_{Q_2}^{(v)} M^{(v)}$ and $Z = F^* F^{*T}$. Eq. (17) is a standard spectral clustering object with graph Laplacian matrix $(\eta Y^{(v)} - \alpha Z)$. By calculating the c eigenvectors of Laplacian matrix corresponding to the c smallest eigenvalues, we can obtain the optimal solution $F^{(v)}$.

Step 2. Updating $A^{(v)}$. Similar to $F^{(v)}$, we have

$$\begin{aligned} A^{(v)} = & (X^{(v)T} X^{(v)} + 2I)^{-1} (X^{(v)T} (X^{(v)} + \frac{H_0^{(v)}}{w_v \theta} - E^{(v)}) \\ & + Q_1^{(v)} + Q_2^{(v)} - \frac{H_1^{(v)}}{w_v \theta} - \frac{H_2^{(v)}}{w_v \theta}). \end{aligned} \quad (18)$$

Since $(X^{(v)T} X^{(v)} + 2I)^{-1}$ is constant, we can pre-compute it before our optimization to reduce the computational cost.

Step 3. Updating $Q_1^{(v)}$. Fixing the other variables, we update $Q_1^{(v)}$ by solving

$$Q_1^{(v)} = \arg \min_{Q_1^{(v)}} \|Q_1^{(v)}\|_G + \frac{w_v \theta}{2} \|Q_1^{(v)} - T^{(v)}\|_F^2, \quad (19)$$

where $T^{(v)} = A^{(v)} + H_1^{(v)} / (w_v \theta)$. Note that $\|Q_1^{(v)}\|_G$ is the nonconvex surrogate of $\text{rank}(Q_1^{(v)})$, and the subproblem of updating $Q_1^{(v)}$ is a nonconvex function. Thus, it is difficult for us to directly obtain a closed-form solution to this problem. Fortunately, based on the Moreau-Yosida regularization technology and difference of convex (DC) programming [44], we can decompose Eq. (20) as the difference of two convex functions to obtain the closed-form solution as follows.

At the $(t+1)$ th iteration ($t > 0$), we update $Q_1^{(v)t+1}$ by solving the following subproblem:

$$Q_1^{(v)t+1} = \arg \min_{Q_1^{(v)t}} \|Q_1^{(v)t}\|_G + \frac{w_v^t \theta}{2} \|Q_1^{(v)t} - T^{(v)t}\|_F^2. \quad (20)$$

To solve Eq. (20), we first develop the following theorem and the corresponding proof.

Theorem 1. Let $\mathbf{T} = \mathbf{U}\Sigma_T\mathbf{V}^T$ be the SVD of \mathbf{T} , where $\Sigma_T = \text{diag}(\sigma_T)$. Set $H(\mathbf{Q}_1^{(v)}) = \|\mathbf{Q}_1^{(v)}\|_G = h \circ \sigma_Q$ be a unitarily invariant function.

$$\min_{\mathbf{Q}_1^{(v)}} H(\mathbf{Q}_1^{(v)}) + \frac{\omega}{2} \|\mathbf{Q}_1^{(v)} - \mathbf{A}\|_F^2. \quad (21)$$

Then an optimal solution to the following problem is $\mathbf{Q}^* = \mathbf{U}\Sigma_Q^*\mathbf{V}^T$, where $\Sigma_Q^* = \text{diag}(\sigma^*)$ and $\sigma^* = \text{prox}_{h,\omega}(\sigma_T)$. $\text{prox}_{h,\omega}(\sigma_T)$ is the Moreau-Yosida operator, defined as

$$\text{prox}_{h,\omega}(\sigma_T) = \arg \min_{\sigma} h(\sigma) + \frac{\omega}{2} \|\sigma - \sigma_T\|_2^2. \quad (22)$$

Proof. Since $\mathbf{T} = \mathbf{U}\Sigma_T\mathbf{V}^T$, then $\Sigma_T = \mathbf{U}^T\mathbf{T}\mathbf{V}$. Denoting $\mathbf{M}^{(v)} = \mathbf{U}^{(v)T}\mathbf{Q}_1^{(v)}\mathbf{V}^{(v)}$ which has exactly the same singular values as $\mathbf{Q}_1^{(v)}$, we have

$$H(\mathbf{Q}_1^{(v)}) + \frac{\omega}{2} \|\mathbf{Q}_1^{(v)} - \mathbf{T}\|_F^2 \quad (23a)$$

$$= H(\mathbf{M}^{(v)}) + \frac{\omega}{2} \|\mathbf{M}^{(v)} - \Sigma_T\|_F^2, \quad (23b)$$

$$\geq H(\Sigma_M^{(v)}) + \frac{\omega}{2} \|\Sigma_M^{(v)} - \Sigma_T\|_F^2, \quad (23c)$$

$$= H(\Sigma_{Q_1}^{(v)}) + \frac{\omega}{2} \|\Sigma_{Q_1}^{(v)} - \Sigma_T\|_F^2, \quad (23d)$$

$$= h(\sigma) + \frac{\omega}{2} \|\sigma - \sigma_T\|_2^2, \quad (23e)$$

$$\geq h(\sigma^*) + \frac{\omega}{2} \|\sigma^* - \sigma_T\|_2^2.$$

Note that Eq. (23b) hold since the Frobenius norm is unitarily invariant; Eq. (23c) is due to the Hoffman-Wielandt inequality; and Eq. (23d) holds as $\Sigma_{Q_1}^{(v)} = \Sigma_M^{(v)}$. Thus, Eq. (23d) is a lower bound of Eq. (23a). Because $\Sigma_M^{(v)} = \Sigma_{Q_1}^{(v)} = \mathbf{Q}_1^{(v)} = \mathbf{U}^{(v)T}\mathbf{M}^{(v)}\mathbf{V}^{(v)}$, the SVD of $\mathbf{M}^{(v)}$ is $\mathbf{M}^{(v)} = \mathbf{U}^{(v)T}\Sigma_M^{(v)}\mathbf{V}^{(v)}$. By minimizing Eq. (23e), we get σ^* . Hence $\mathbf{M}^* = \mathbf{U}\text{diag}(\sigma^*)\mathbf{V}^T$, which is the optimal solution of Eq. (21). Thus, Theorem 1 is proved. \square

Note that $\|\mathbf{Q}_1^{(v)}\|_G$ is the nonconvex surrogate of $\text{rank}(\mathbf{Q}_1^{(v)})$, and the subproblem of updating $\mathbf{Q}_1^{(v)}$ is a non-convex function. Thus, it is difficult for us to directly obtain a closed-form solution to this problem. Fortunately, based on the Moreau-Yosida regularization technology and difference of convex (DC) programming [44], we can decompose Eq. (20) as the difference of two convex functions and iteratively optimizes it by linearizing the concave term at each iteration. For the $(t+1)$ th iteration, we have

$$\sigma^{t+1} = \arg \min h(\sigma^t) + \frac{\omega^t}{2} \|\sigma^t - \sigma_T^t\|_2^2, \quad (24)$$

which admits a closed-form solution [45]

$$\sigma^{t+1} = (\sigma_T^t - \frac{\varphi_t}{\omega^t})_+, \quad (25)$$

where $\varphi_t = \partial h(\sigma^t)$ is the gradient of $h(\cdot)$ at σ^t , and $\mathbf{U}^{(v)}\text{diag}(\sigma_T^t)^{(v)}\mathbf{V}^{(v)T}$ is the SVD of $(\mathbf{A}^{(v)} + \mathbf{H}_1^{(v)})/(w_v\theta)$. After a number of iterations, it converges to a local optimal point σ^* . Then $\mathbf{Q}_1^{(v)t+1} = \mathbf{U}^{(v)}\text{diag}(\sigma^{(v)*})\mathbf{V}^{(v)T}$.

Step 4. Updating $\mathbf{Q}_2^{(v)}$. Similar to $\mathbf{F}^{(v)}$ and [35], we can update $\mathbf{Q}_2^{(v)}$ as follows:

$$\mathbf{Q}_{2,i,j}^{(v)} = \begin{cases} \mathbf{R}_{i,:}^{(v)} - \frac{\eta}{2w_v\theta} \mathbf{S}_{i,:}^{(v)}, & \text{if } \mathbf{R}_{i,:}^{(v)} \geq \frac{\eta}{2w_v\theta} \mathbf{S}_{i,:}^{(v)}; \\ \mathbf{R}_{i,:}^{(v)} + \frac{\eta}{2w_v\theta} \mathbf{S}_{i,:}^{(v)}, & \text{if } \mathbf{R}_{i,:}^{(v)} < \frac{\eta}{2w_v\theta} \mathbf{S}_{i,:}^{(v)}, \end{cases} \quad (26)$$

where $\mathbf{S}_{i,j}^{(v)} = \|\mathbf{G}_{i,:}^{(v)} - \mathbf{G}_{j,:}^{(v)}\|_2^2$, $\mathbf{G}_{i,:}^{(v)}$ and $\mathbf{G}_{j,:}^{(v)}$ is the i -th and j -th row vectors of $\mathbf{G}^{(v)}$, respectively. $\mathbf{R}_{i,:}^{(v)} = \mathbf{A}_{i,:}^{(v)} + \mathbf{H}_{2,i,:}^{(v)}/(w_v\theta)$ and $\mathbf{G}^{(v)} = \mathbf{M}^{(v)}\mathbf{F}^{(v)}$.

Step 5. Updating $\vartheta^{(v)}$. Due to $\mathbf{Q}_{2,i,:}^{(v)} \mathbf{1} = \mathbf{1}$ with Eq. (26), the Lagrange multiplier can be updated as follows:

$$\vartheta_i^{(v)} = \frac{w_v\theta(\sum_{i,j}(\mathbf{Q}_{2,i,j}^{(v)} - \frac{\mathbf{H}_{2,i,i}^{(v)}}{w_v\theta}) - 1)}{1 - n_v}. \quad (27)$$

Step 6. Updating $\mathbf{E}^{(v)}$. Similar to $\mathbf{F}^{(v)}$, we update $\mathbf{E}^{(v)}$ as follows:

$$\mathbf{E}^{(v)} = (\frac{\beta}{w_v\theta} \mathbf{D}^{(v)} + \mathbf{I})^{-1} \mathbf{K}^{(v)}, \quad (28)$$

where $\mathbf{D}^{(v)} = \partial \|\mathbf{E}^{(v)}\|_{2,1} / \partial \mathbf{E}^{(v)} \mathbf{E}^{(v)-1}$, $\mathbf{K}^{(v)} = \mathbf{X}^{(v)} - \mathbf{X}^{(v)}\mathbf{A}^{(v)} + \mathbf{H}_0^{(v)}/(w_v\theta)$.

Step 7. Updating \mathbf{F}^* . Similar to $\mathbf{F}^{(v)}$, we minimize the following objective function:

$$\begin{aligned} & -\alpha \text{Tr}(\mathbf{F}^* \mathbf{F}^{*T} \mathbf{F}^{(v)} \mathbf{F}^{(v)T}) \\ \implies & \text{Tr}(\mathbf{F}^{*T} (-\mathbf{F}^{(v)} \mathbf{F}^{(v)T}) \mathbf{F}^*). \end{aligned} \quad (29)$$

We can obtain the optimal solution $\mathbf{F}^{(v)}$ by calculating the c eigenvectors of $\sum_v (\mathbf{F}^{(v)} \mathbf{F}^{(v)T})$ corresponding to the c largest eigenvalues.

Step 8. Updating $\mathbf{H}_0^{(v)}, \mathbf{H}_1^{(v)}, \mathbf{H}_2^{(v)}$. Similar to $\mathbf{F}^{(v)}$, we update $\mathbf{H}_0^{(v)}, \mathbf{H}_1^{(v)}$ and $\mathbf{H}_2^{(v)}$ by

$$\begin{aligned} \mathbf{H}_0^{(v)} &= \mathbf{H}_0^{(v)} + w_v\theta(\mathbf{X}^{(v)} - \mathbf{X}^{(v)}\mathbf{A}^{(v)} - \mathbf{E}^{(v)}) \\ \mathbf{H}_1^{(v)} &= \mathbf{H}_1^{(v)} + w_v\theta(\mathbf{A}^{(v)} - \mathbf{Q}_1^{(v)}) \\ \mathbf{H}_2^{(v)} &= \mathbf{H}_2^{(v)} + w_v\theta(\mathbf{A}^{(v)} - \mathbf{Q}_2^{(v)}). \end{aligned} \quad (30)$$

Step 9. Updating w_v . Fixing the other variables, we update w_v by Eq. (9).

F. Convergence Analysis

Note that the optimization of UIMC is simplified as nine steps. Each step can obtain the closed solution w.r.t. the corresponding variable. The objective function is bounded and all the above nine steps do not increase the objective function value. For Step 1, Step 2, and Step 4-9, we can easily find their objective functions are bounded and these steps do not increase the objective function value. Therefore, we try to analyze the impact of Step 3 on the objective function in our submission.

For convenience, we write $\|\mathbf{Q}_1^{(v)}\|_G$ as $H(\mathbf{Q}_1^{(v)})$ in Eq. (16) in our submission.

$$\begin{aligned} J(\mathbf{Q}_1^{(v)}, \mathbf{A}^{(v)}, \mathbf{H}_1^{(v)}, w_v) &= \sum_v (H(\mathbf{Q}_1^{(v)}) \\ &+ \frac{w_v\theta}{2} \|\mathbf{A}^{(v)} - \mathbf{Q}_1^{(v)}\|_F^2 + < \frac{\mathbf{H}_1^{(v)}}{w_v\theta}, \mathbf{A}^{(v)} - \mathbf{Q}_1^{(v)} >), \end{aligned} \quad (31)$$

where $\langle \cdot, \cdot \rangle$ is the inner product of two matrices [46].

Lemma 2. $Q_1^{(v)^t}$ is bounded.

Proof. With some algebra, we can obtain

$$\begin{aligned} & J(Q_1^{(v)^t}, A^{(v)^t}, H_1^{(v)^t}, w_v^t) \\ &= J(Q_1^{(v)^t}, A^{(v)^t}, H_1^{(v)^{t-1}}, w_v^{t-1}) \\ & \quad + \frac{(w_v^t - w_v^{t-1})\theta}{2} \|A^{(v)} - Q_1^{(v)}\|_F^2 \\ & \quad + \text{Tr}[(H_1^{(v)^t} - H_1^{(v)^{t-1}})(A^{(v)} - Q_1^{(v)})] \\ &= J(Q_1^{(v)^t}, A^{(v)^t}, H_1^{(v)^{t-1}}, w_v^{t-1}) \\ & \quad + \frac{w_v^t + w_v^{t-1}}{2\theta(w_v^{t-1})^2} \|H_1^{(v)^t} - H_1^{(v)^{t-1}}\|_F^2. \end{aligned} \quad (32)$$

Then,

$$\begin{aligned} & J(Q_1^{(v)^{t+1}}, A^{(v)^{t+1}}, H_1^{(v)^t}, w_v^t) \\ & \leq J(Q_1^{(v)^{t+1}}, A^{(v)^t}, H_1^{(v)^t}, w_v^t) \\ & \leq J(Q_1^{(v)^t}, A^{(v)^t}, H_1^{(v)^t}, w_v^t) \\ & \leq J(Q_1^{(v)^t}, A^{(v)^t}, H_1^{(v)^{t-1}}, w_v^{t-1}) \\ & \quad + \frac{w_v^t + w_v^{t-1}}{2\theta(w_v^{t-1})^2} \|H_1^{(v)^t} - H_1^{(v)^{t-1}}\|_F^2. \end{aligned} \quad (33)$$

Iterating the inequality chain (33) t times, we obtain

$$\begin{aligned} & J(Q_1^{(v)^{t+1}}, A^{(v)^{t+1}}, H_1^{(v)^t}, w_v^t) \\ & \leq J(Q_1^{(v)^1}, A^{(v)^1}, H_1^{(v)^0}, w_v^0) \\ & \quad + \sum_{i=1}^t \frac{w_v^i + w_v^{i-1}}{2\theta(w_v^{i-1})^2} \|H_1^{(v)^i} - H_1^{(v)^{i-1}}\|_F^2 \end{aligned} \quad (34)$$

Based on the definition of w_v and θ in our submission, we have $\sum_{i=1}^{\infty} (w_v^i + w_v^{i-1}) / (2\theta(w_v^{i-1})^2) < \infty$. Since $\|H_1^{(v)^i} - H_1^{(v)^{i-1}}\|_F^2$ is bounded, all terms on the righthand side of the above inequality are bounded, thus $J(Q_1^{(v)^{t+1}}, A^{(v)^{t+1}}, H_1^{(v)^t}, w_v^t)$ is upper bounded.

Besides,

$$\begin{aligned} & J(Q_1^{(v)^{t+1}}, A^{(v)^{t+1}}, H_1^{(v)^t}, w_v^t) + \frac{1}{2\theta w_v^t} \|H_1^{(v)^t}\|_F^2 \\ &= H(Q_1^{(v)^{t+1}}) + \frac{w_v\theta}{2} \|A^{(v)^{t+1}} - Q_1^{(v)^{t+1}}\|_F^2 + \frac{H_1^{(v)^t}}{w_v\theta} \|A^{(v)^{t+1}} - Q_1^{(v)^{t+1}}\|_F^2. \end{aligned} \quad (35)$$

Since each term on the right-hand side is bounded, $A^{(v)^{t+1}}$ is bounded. By the last term on the right-hand of Eq. (35), $\{Q_1^{(v)^t}\}$ is bounded. Therefore, both $\{Q_1^{(v)^t}\}$ and $\{A^{(v)^t}\}$ are bounded. \square

Lemma 3. Let $\{Q_1^{(v)^t}, A^{(v)^t}, H_1^{(v)^t}\}$ be the sequence and $\{Q_1^{(v)*}, A^{(v)*}, H_1^{(v)*}\}$ be an accumulation point. Then $\{Q_1^{(v)*}, A^{(v)*}\}$ is a stationary point if $\lim_{t \rightarrow \infty} w_v^t (A^{(v)^{t+1}} - A^{(v)^t}) \rightarrow 0$.

Proof. The sequence $\{Q_1^{(v)^t}, Z^{(v)^t}, H_1^{(v)^t}\}$ is bounded as shown in Lemma 3. By Bolzano-Weierstrass theorem, the sequence must have at least one accumulation point, e.g., $\{Q_1^{(v)*}, A^{(v)*}, H_1^{(v)*}\}$. Without loss of generality,

TABLE I: Statistics of datasets.

Dataset	BUAA	3-Sources	BBC	Digit
# views	2	3	4	5
# instances	180	169	685	2000
# clusters	20	6	5	10

we assume that $\{Q_1^{(v)^t}, A^{(v)^t}, H_1^{(v)^t}\}$ itself converges to $\{Q_1^{(v)*}, A^{(v)*}, H_1^{(v)*}\}$.

Since $A^{(v)^t} - Q_1^{(v)^t} = (H_1^{(v)^t} - H_1^{(v)^{t-1}}) / (w_v^t \theta)$, we have $\lim_{t \rightarrow \infty} A^{(v)^t} - Q_1^{(v)^t} = 0$. Thus the primal feasibility condition is satisfied.

For $Q_1^{(v)^{t+1}}$, it is true that

$$\begin{aligned} & \partial_{Q_1} (Q_1^{(v)^{t+1}}, A^{(v)^t}, H_1^{(v)^t}, w_v^t) \big|_{Q_1^{(v)^{t+1}}} \\ &= \partial_{Q_1} H(Q_1^{(v)^{t+1}}) + H_1^{(v)^t} + w_v^t \theta (A^{(v)^t} - Q_1^{(v)^t}) \\ &= \partial_{Q_1} H(Q_1^{(v)^{t+1}}) + H_1^{(v)^{t+1}} + w_v^t \theta (A^{(v)^{t+1}} - A^{(v)^t}) = 0. \end{aligned} \quad (36)$$

If the singular value decomposition of $Q_1^{(v)}$ is $U^{(v)} \text{diag}(\sigma_i^{(v)}) V^{(v)T}$, according to Theorem 1,

$$\partial_{Q_1} H(Q_1^{(v)^{t+1}}) \big|_{Q_1^{(v)^{t+1}}} = U \text{diag}(\tau^{(v)}) V^{(v)T}, \quad (37)$$

where $\tau_i = \gamma / (\gamma + \sigma_i)^2$ if $\sigma_i \neq 0$; otherwise, it is $1/\gamma$. Since $\sigma_i \in (0, 1/\gamma]$ is finite, $H(Q_1^{(v)^{t+1}}) \big|_{Q_1^{(v)^{t+1}}}$ is bounded. Since $A^{(v)^t}$ is bounded, $w_v^t \theta (A^{(v)^{t+1}} - A^{(v)^t})$ is bounded. Under the assumption that $w_v^t \theta (A^{(v)^{t+1}} - A^{(v)^t}) \rightarrow 0$,

$$\partial_{Q_1} H(Q_1^{(v)^{t+1}}) \big|_{Q_1^{(v)^{t+1}}} + H_1^{(v)*} = 0. \quad (38)$$

Hence, $\{Q_1^{(v)*}, A^{(v)*}, H_1^{(v)*}\}$ satisfies the KKT conditions of $J(Q_1^{(v)^{t+1}}, Z^{(v)^{t+1}}, H_1^{(v)^t})$. Thus $\{Q_1^{(v)*}, A^{(v)*}\}$ is a stationary point of the objective function. \square

Thus, the objective function can reduce monotonically to a stationary value and UIMC can at least find a locally optimal solution. When we initialize each variable to obtain this solution, different initialization methods may affect the convergence speed, but UIMC will eventually reach convergence due to the monotonic decline of our objective function.

IV. PERFORMANCE EVALUATION

We first illustrate the clustering performance of the proposed UIMC, then verify UIMC's convergence, and finally analyze UIMC's parameter sensitivity.

A. Datasets

We conduct experiments on four real-world multi-view datasets (shown in Table I) as follows: BUAA dataset [47], 3-Sources dataset², BBC dataset³, and Digit dataset⁴.

1) BUAA-visnir face dataset (BUAA): BUAA has 90 visual images and 90 near infrared images (i.e., 180 instances), which are categorized into 10 classes (i.e., 10 clusters). Each image is described by two views: VIS and NIR.

²<http://erdos.ucd.ie/datasets/3sources.html>.

³<http://mlg.ucd.ie/datasets/segment.html>.

⁴<http://archive.ics.uci.edu/ml/datasets/Multiple+Features>.

TABLE II: The missing rate vector of each view.

BUAA	3-Sources	BBC	Digit
VIS ($1 \times r$)	BBC ($0.2 \times r$)	Ba ($0.25 \times r$)	FAC ($0.25 \times r$)
NIR ($1 \times r$)	REU ($1.0 \times r$)	Bb ($0.75 \times r$)	FOU ($0.75 \times r$)
-	GUA ($1.8 \times r$)	Bc ($1.25 \times r$)	KAR ($1.00 \times r$)
-	-	Bd ($1.75 \times r$)	PIX ($1.25 \times r$)
-	-	-	ZER ($1.75 \times r$)

2) 3 Sources dataset (**3 Sources**): 3-Sources contains 948 news articles collected from three online news sources (i.e., 3 views): BBC, Reuters (REU), and The Guardian (GUA). We select a subset with 169 articles (i.e., 169 instances), which are categorized into 6 topical labels (i.e., 6 clusters).

3) BBC dataset (**BBC**): BBC is collected from the BBC news website consisting of 685 documents (i.e., 685 instances). Each document was split into four segments (i.e., View a, View b, View c, and View d) and was manually annotated with one of five topical labels (i.e., 5 clusters).

4) Handwritten digit dataset (**Digit**): Digit contains 2000 handwritten numerals (i.e., 2000 instances) collected from the following views: (i) 216 profile correlations (FAC), (ii) 76 Fourier coefficients of the character shapes (FOU), (iii) 64 Karhunen-Love coefficients (KAR), (iv) 240 pixel averages in 2×3 windows (PIX), (v) 47 Zernike moments (ZER).

Data preprocessing: To obtain incomplete multi-view data for clustering, we need to preprocess the real data. Following [21], we randomly delete some instances from each view to obtain incomplete views. For an incomplete multi-view dataset, we denote its average missing rate⁵ as PER, and we set different PERs from 0 to 0.5. To describe the missing rate of each view, we define a missing rate vector $r=[0, 0.1, 0.2, \dots, 0.5]$, which represents a series of average missing rates (from PER=0 to PER=0.5). The missing rate vector of each view is shown in Table II. For example, for 3-Sources dataset, when the average missing rate PER=0.1, the missing rate of GUA is $1.8 \times 0.1=0.18$.

B. Compared Methods

We compare our proposed UIMC with following eight state-of-the-art methods, which are the most relevant to our work: (a) **BSV** (Best Single View) [27] first fills in the missing views with the average of instances in the corresponding view, then perform K-means clustering on each view separately, and finally we report the best clustering result; (b) **Concat** [27], same as BSV, first fills in all the missing data, then concatenates all views into one single view, and finally performs K-means clustering on the single view; (c) **PVC** [26] establishes a latent subspace to align two incomplete views; (d) **IMG** [27] extends PVC by introducing manifold learning; (e) **MIC** [28] extends MultiNMF via weighted NMF and $L_{2,1}$ regularization; (f) **DAIMC** [21] extends MIC via weighted semiNMF and $L_{2,1}$ -norm regularization regression; (g) **IMSC_AGL** [30] learns the common representation by exploiting the graph learning and spectral clustering; (h) **UEAF** [34] performs clustering by aligning the unified common embedding. Concat is the baseline method in our experiments.

⁵The average missing rate is the average of the missing rates of all views.

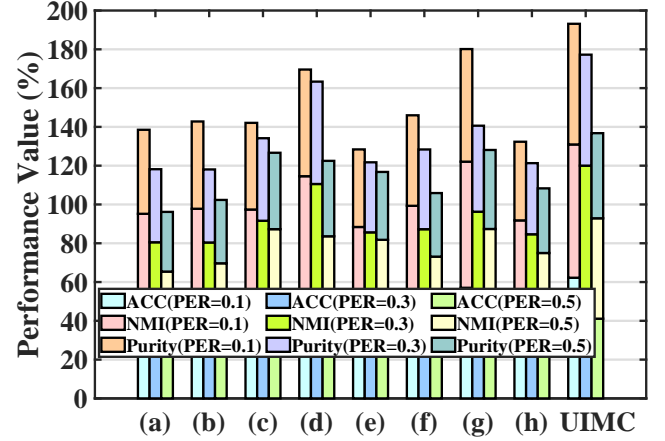


Fig. 3: Balanced incomplete multi-view clustering results, where (a) is BSV, (b) is Concat, (c) is PVC, (d) is IMG, (e) is MIC, (f) is DAIMC, (g) is IMSC_AGL, (h) is UEAF.

All results of compared methods are produced by released codes, some of which may be inconsistent with published information due to different pretreatment processes. All the codes in our experiments are implemented in MATLAB R2020b and run on a Windows 10 machine with 3.30 GHz E3-1225 CPU, 64 GB main memory. We perform the following two types of experiments:

- 1) Balanced incomplete multi-view clustering on BUAA dataset: We compare UIMC with all the above methods.
- 2) Unbalanced incomplete multi-view clustering on 3-Sources, BBC and Digit datasets: Note that MIC, DAIMC, IMSC_AGL, and UEAF cannot cluster unbalanced incomplete multi-view datasets. For each dataset, similar to Concat, we concatenate all incomplete views into one view, and perform these methods on the single view. Since PVC and IMG are based on two views (neither one view nor more than two views), we do not compare UIMC with PVC and IMG here. For three parameters in UIMC, we set $\alpha=10^{-2}$, $\beta=10^5$, and $\eta=10^{-1}$.

Evaluation metrics: Following [26], we repeat each experiment 10 times and report the average clustering results. Following [30], [34], we evaluate the results by three popular clustering evaluation metrics: accuracy (ACC), normalized mutual information (NMI), and Purity. For these evaluation metrics, the larger value represents the better clustering performance.

C. Experimental Results and Analysis

Fig. 3 shows the balanced incomplete multi-view clustering results and Fig. 4 gives the unbalanced incomplete multi-view clustering results. Obviously, UIMC performs best on all datasets, which shows that UIMC is not sensitive to the dataset. All the results show that our proposed UIMC outperforms the compared methods on all datasets, which shows that UIMC is not sensitive to the dataset. Impressively, compared with the best performing method among compared methods on Digit dataset with PER=0.4 (Fig. 4(g)-4(i)), UIMC at least raises ACC by 44.50%, NMI by 42.70%, purity by 43.15%.

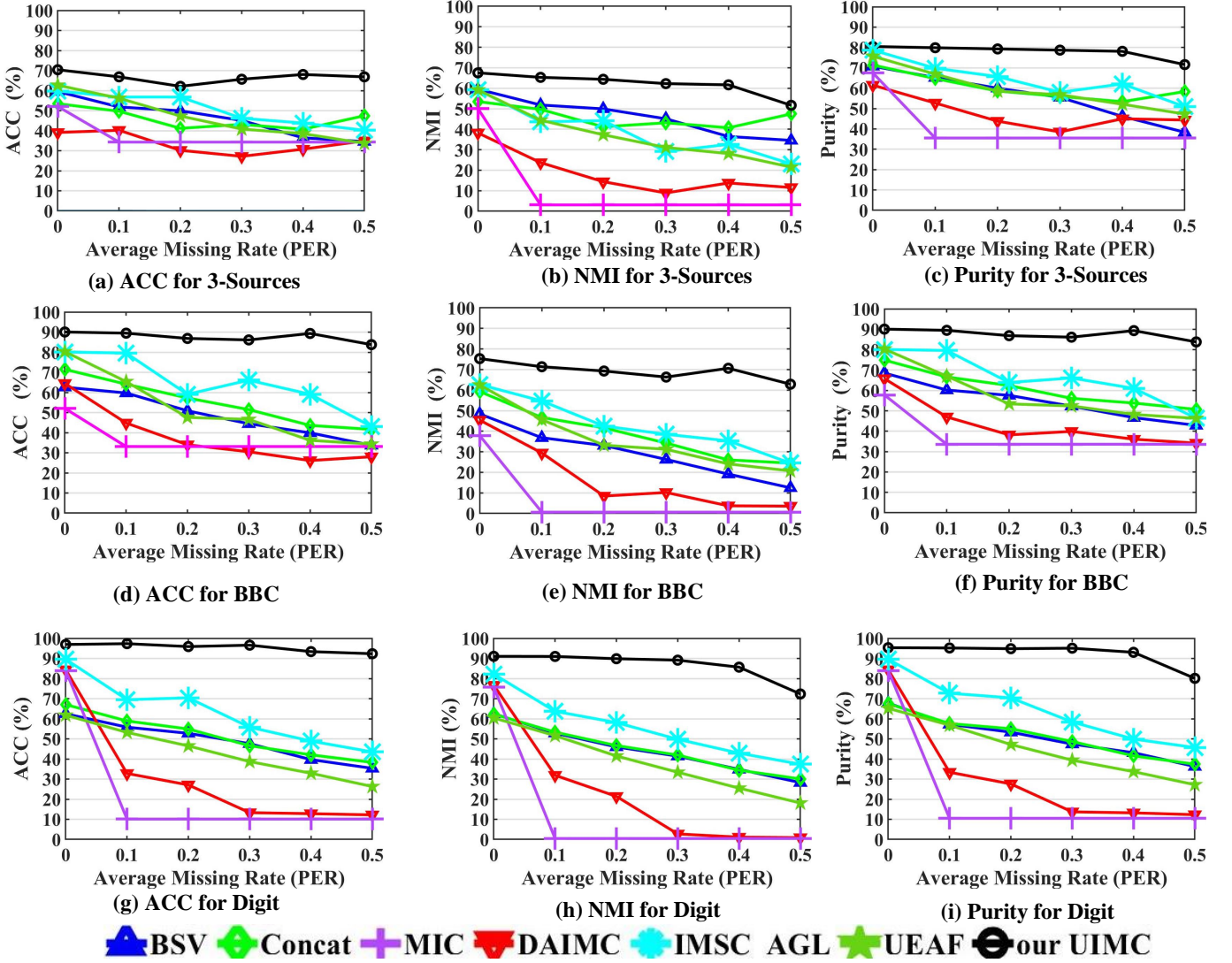


Fig. 4: Unbalanced incomplete multi-view clustering results.

1) Balanced incomplete multi-view clustering: In Fig. 3, our proposed UIMC outperforms all the compared methods significantly for all missing rates. Specifically, relative to the compared methods, UIMC at least improves clustering performance (ACC+NMI+Purity) by 17.63% with PER=0.1, by 15.42% with PER=0.3, by 11.06% with PER=0.5. It is mainly because based on $L_{2,1}$ -norm, UIMC can learn the robust representation to decrease the influence of noises in BUAA. Also, the superior improvement proves that UIMC performs better than other state-of-the-art methods on balanced incomplete multi-view clustering tasks. Compared with PVC, IMG raises clustering results when PER=0.1 and PER=0.3. The reason is that based on a graph Laplacian term, IMG can learn the global structure. Obviously, UIMC obtains better clustering performance because UIMC aligns two incomplete views by minimizing the disagreement between their cluster indicator matrix and the consensus. This shows that UIMC can handle balanced incomplete multi-view clustering tasks more effectively than the other state-of-the-art methods.

2) Unbalanced incomplete multi-view clustering: In Fig. 4,

our proposed UIMC also obtains better performance than other state-of-the-art methods on three datasets for unbalanced incomplete clustering. As the PER increases, the clustering results of other methods drop sharply, but UIMC still keeps satisfactory clustering performance due to our proposed weighted MVSC. The main reason is that UIMC can cover these data with the help of Γ -norm, which decreases the influence of incompleteness. Interestingly, comparing the performance improvement of UIMC on 3-Sources, BBC and Digit datasets, we find that UIMC has the largest improvement on BBC and the least improvement on Digit. It is because UIMC weights each view based on its incompleteness, which makes full use of these presented instances for clustering. When PER>0, both MIC and DAIMC perform worse than BSV and Concat. It is because MIC and DAIMC rely on view alignment but they cannot align different views after concatenating all views. This also shows that it is invalid to solve the unbalanced incomplete multi-view clustering problem by concatenating all the views. Compared with Concat, IMSC_AGL and UEAF have a small improvement. For example, when clustering BBC dataset with

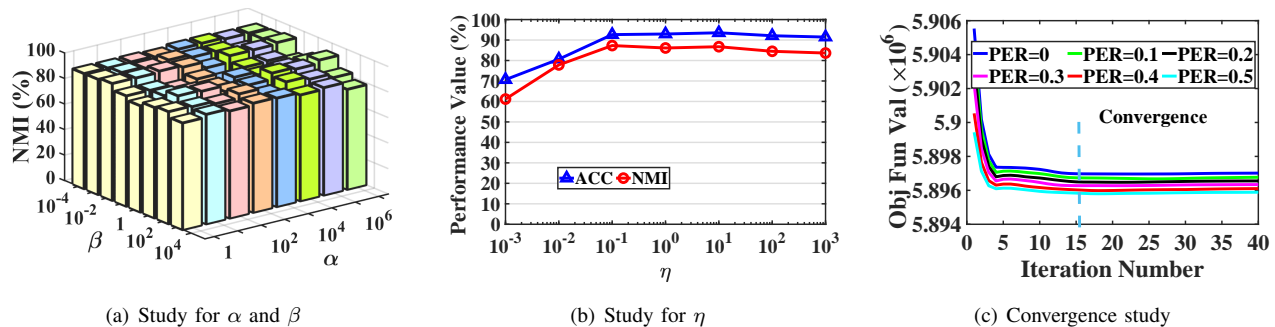


Fig. 5: Parameter sensitivity and convergence study

PER=0.2, IMSC_AGL and UEAF improve clustering results by up to 10%, while our proposed UIMC improves the performance by at least 30%. The large improvements show that UIMC effectively solves unbalanced incomplete multi-view clustering problem. The reason is that UIMC effectively bridges these incomplete views by constructing the Laplacian graphs with the same matrix size.

D. Parameter Sensitivity and Convergence Study

We analyze hyper-parameters (α , β , and η) by conducting experiments for our proposed UIMC on Digit dataset. We set PER=0.3 and report the clustering performance of UIMC versus α , β and η . From Fig. 5(a) and 5(b), as these parameters change, UIMC keeps stable and satisfactory clustering performance. It illustrates that UIMC is insensitive to these parameters to some extent. Besides, UIMC obtains the best clustering results when $\alpha=10^{-2}$, $\beta=10^5$, and $\eta=10^{-1}$, which are our recommended values.

We study UIMC's convergence by experimenting on BBC dataset with different PERs. We set the hyper-parameters α, β, η as $10^{-2}, 10^5, 10^{-1}$, respectively. Fig. 5(c) shows that the convergence curve versus the number of iterations, where "Obj Fun Val" donates "Objective function value". The blue dashed line indicates the convergence of the objective function. It can be seen that UIMC has converged just after 16 iterations for all PERs, which verifies the convergence of UIMC. Most incomplete multi-view clustering works (e.g., DAIMC) state that their methods converge after 30 iterations. Compared with these methods, our UIMC can reach convergence faster.

V. CONCLUSION

In this paper, we propose a novel unbalanced incomplete multi-view clustering method, named as UIMC. To our best knowledge, it presents the first effective method to cluster multiple views with different incompleteness. Inspired by the biological evolution theory, we propose the scheme of view evolution to integrate these unbalanced incomplete views for clustering. After each iteration of optimization, the weights of strong views increase, while the weights of the weak views decrease. Extensive experiments on four real-world multi-view datasets show the superior performance gain and effectiveness of UIMC. Impressively, compared with the baseline method Concat on the Digit dataset with the missing rate of 0.4, other

state-of-the-art methods at least improve ACC by 5.20%, NMI by 7.33% and purity by 8.30%, while our proposed UIMC at least improves ACC by 51.35%, NMI by 51.26% and purity by 51.20%.

REFERENCES

- [1] Y. Ong and A. Gupta, "Air5: Five pillars of artificial intelligence research," *IEEE TETCI*, pp. 411–415, 2019.
- [2] C. Du, C. Du, X. Xie, C. Zhang, and H. Wang, "Multi-view adversarially learned inference for cross-domain joint distribution matching," in *SIGKDD*. ACM, 2018, pp. 1348–1357.
- [3] Y. Feng, P. Zhou, D. Wu, and Y. Hu, "Accurate content push for content-centric social networks: A big data support online learning approach," *IEEE TETCI*, pp. 426–438, 2018.
- [4] Q. Zhang, Z. Sun, W. Hu, M. Chen, L. Guo, and Y. Qu, "Multi-view knowledge graph embedding for entity alignment," *arXiv preprint*, 2019.
- [5] C. Gong, D. Tao, S. J. Maybank, W. Liu, G. Kang, and J. Yang, "Multi-modal curriculum learning for semi-supervised image classification," *TIP*, pp. 3249–3260, 2016.
- [6] K. Muhammad, M. Sajjad, I. Mehmood, S. Rho, and S. W. Baik, "A novel magic lsb substitution method (m-lsb-sm) using multi-level encryption and achromatic component of an image," *Multimedia Tools & Applications*, pp. 1–27, 2016.
- [7] S. Wen, H. Wei, Z. Zeng, and T. Huang, "Memristive fully convolutional network: An accurate hardware image-segmentor in deep learning," *IEEE TETCI*, pp. 324–334, 2018.
- [8] Z. Lu and Y. Peng, "Unified constraint propagation on multi-view data," in *AAAI*, 2013.
- [9] X. He, M.-Y. Kan, P. Xie, and X. Chen, "Comment-based multi-view clustering of web 2.0 items," in *WWW*, 2014, pp. 771–782.
- [10] A. Gupta, Y. Ong, and L. Feng, "Insights on transfer optimization: Because experience is the best teacher," *IEEE TETCI*, pp. 51–64, 2018.
- [11] L. Gao, H. Yang, J. Wu, C. Zhou, W. Lu, and Y. Hu, "Recommendation with multi-source heterogeneous information," in *IJCAI*, 2018.
- [12] J. Gao, X. Wang, Y. Wang, and X. Xie, "Explainable recommendation through attentive multi-view learning," in *AAAI*, 2019, pp. 3622–3629.
- [13] Z. Zhang, L. Liu, F. Shen, H. T. Shen, and L. Shao, "Binary multi-view clustering," *IEEE TPAMI*, pp. 1774–1782, 2019.
- [14] Y. Li, C. Pan, X. Cao, and D. Wu, "Power line detection by pyramidal patch classification," *IEEE TETCI*, pp. 416–426, 2019.
- [15] T. He, Y. Liu, T. H. Ko, K. C. C. Chan, and Y. S. Ong, "Contextual correlation preserving multiview featured graph clustering," *IEEE Transactions on Cybernetics*, pp. 4318–4331, 2020.
- [16] A. Blum and T. Mitchell, "Combining labeled and unlabeled data with co-training," in *COLT*. ACM, 1998, pp. 92–100.
- [17] S. Li, M. Shao, and Y. Fu, "Multi-view low-rank analysis with applications to outlier detection," *ACM TKDD*, pp. 1–22, 2018.
- [18] C. Tang, X. Zhu, X. Liu, and L. Wang, "Cross-view local structure preserved diversity and consensus learning for multi-view unsupervised feature selection," in *AAAI*, 2019.
- [19] X. Peng, Z. Huang, J. Lv, H. Zhu, and J. T. Zhou, "COMIC: Multi-view clustering without parameter selection," in *ICML*, 2019, pp. 5092–5101.
- [20] Y. Liu, Y. Zheng, Y. Liang, S. Liu, and D. S. Rosenblum, "Urban water quality prediction based on multi-task multi-view learning," in *IJCAI*, 2016, pp. 2576–2582.

- [21] M. Hu and S. Chen, "Doubly aligned incomplete multi-view clustering," in *IJCAI*, 2018, pp. 2262–2268.
- [22] H. Li, J. Zhang, and C. Zong, "Implicit discourse relation recognition for english and chinese with multiview modeling and effective representation learning," *TALLIP*, p. 19, 2017.
- [23] Y. Wang, L. Zhou, J. Zhang, F. Zhai, J. Xu, C. Zong *et al.*, "A compact and language-sensitive multilingual translation method," pp. 1213–1223, 2019.
- [24] H. Wang, B. Chen, and W.-J. Li, "Collaborative topic regression with social regularization for tag recommendation," in *IJCAI*, 2013.
- [25] W. Min, S. Jiang, S. Wang, J. Sang, and S. Mei, "A delicious recipe analysis framework for exploring multi-modal recipes with various attributes," in *ACM MM*, 2017, pp. 402–410.
- [26] S.-Y. Li, Y. Jiang, and Z.-H. Zhou, "Partial multi-view clustering," in *AAAI*, 2014.
- [27] H. Zhao, H. Liu, and Y. Fu, "Incomplete multi-modal visual data grouping," in *IJCAI*, 2016, pp. 2392–2398.
- [28] W. Shao, L. He, and S. Y. Philip, "Multiple incomplete views clustering via weighted nonnegative matrix factorization with $l_{2,1}$ regularization," in *ECML_PKDD*. Springer, 2015, pp. 318–334.
- [29] D. D. Lee and H. S. Seung, "Learning the parts of objects by non-negative matrix factorization," *Nature*, vol. 401, no. 6755, p. 788, 1999.
- [30] J. Wen, Y. Xu, and H. Liu, "Incomplete multiview spectral clustering with adaptive graph learning," *IEEE transactions on cybernetics*, 2019.
- [31] F. Nie, J. Li, X. Li *et al.*, "Self-weighted multiview clustering with multiple graphs," in *IJCAI*, 2017, pp. 2564–2570.
- [32] L. Zong, X. Zhang, X. Liu, and H. Yu, "Weighted multi-view spectral clustering based on spectral perturbation," in *AAAI*, 2018.
- [33] F. Nie, G. Cai, J. Li, and X. Li, "Auto-weighted multi-view learning for image clustering and semi-supervised classification," *TIP*, pp. 1501–1511, 2018.
- [34] J. Wen, Z. Zhang, Y. Xu, B. Zhang, L. Fei, and H. Liu, "Unified embedding alignment with missing views inferring for incomplete multi-view clustering," in *AAAI*, 2019, pp. 5393–5400.
- [35] H. Gao, F. Nie, X. Li, and H. Huang, "Multi-view subspace clustering," in *CVPR*, 2015, pp. 4238–4246.
- [36] H. Spencer, *The principles of biology*. Appleton, 1875, vol. 2.
- [37] C. Darwin, *On the origin of species, 1859*. Routledge, 2004.
- [38] D. Mitchell, *Cloud atlas*. Hachette UK, 2008.
- [39] C. Zhang, Q. Hu, H. Fu, P. Zhu, and X. Cao, "Latent multi-view subspace clustering," in *CVPR*, 2017, pp. 4279–4287.
- [40] H. Yin, X. Zhang, T. Zhan, Y. Zhang, G. Min, and D. O. Wu, "Netclust: A framework for scalable and pareto-optimal media server placement," *IEEE TMM*, pp. 2114–2124, 2013.
- [41] T. Qiu, A. Zhao, F. Xia, W. Si, and D. O. Wu, "Rose: Robustness strategy for scale-free wireless sensor networks," *IEEE/ACM Transactions on Networking*, pp. 2944–2959, 2017.
- [42] L. Zhu, J. Zhang, Z. Xiao, X. Cao, D. O. Wu, and X. Xia, "Millimeter-wave noma with user grouping, power allocation and hybrid beamforming," *IEEE TWC*, pp. 5065–5079, 2019.
- [43] Z. Kang, C. Peng, and Q. Cheng, "Robust pca via nonconvex rank approximation," in *ICDM*, 2015, pp. 211–220.
- [44] P. D. Tao and L. T. H. An, "Convex analysis approach to dc programming: theory, algorithms and applications," *Acta mathematica vietnamica*, vol. 22, no. 1, pp. 289–355, 1997.
- [45] W. Zhang, Y. Wen, K. Guan, D. Kilper, H. Luo, and D. O. Wu, "Energy-optimal mobile cloud computing under stochastic wireless channel," *IEEE TWC*, pp. 4569–4581, 2013.
- [46] C. Xu, J. Zhu, and D. O. Wu, "Decentralized online learning methods based on weight-balancing over time-varying digraphs," *IEEE TETCI*, pp. 1–13, 2018.
- [47] D. Huang, J. Sun, and Y. Wang, "The buaa-visnir face database instructions," *School Comput. Sci. Eng., Beihang Univ., Beijing, China, Tech. Rep. IRIP-TR-12-FR-001*, 2012.